MECHANIKA TEORETYCZNA
I STOSOWANA
Journal of Theoretical
and Applied Mechanics
2, 35, 1997

GODUNOV-TYPE SCHEMES IN THE TRANSONIC FLOW CALCULATIONS

TADEUSZ CHMIELNIAK

WŁODZIMIERZ WRÓBLEWSKI

Institute of Power Machinery, Silesian Technical University

e-mail: wroblews@zeus.polsl.gliwice.pl

An explicit, time marching solvers for the calculation of the three dimensional Euler equations and two-dimensional compressible Navier-Stokes equations are described. The equations are discretized spatially by a node-centered finite volume formulation. To make the present approach robust, the inviscid fluxes at cell interfaces are evaluated using a high accurate TVD scheme based on the MUSCL-type technique with the Riemann solvers. The Baldwin-Lomax eddy-viscosity model for the turbulence calculation is used. The calculations are performed using "C"-type and "H"-type grids. The numerical results are reported, compared with experimental data and discussed.

Key words: transonic flow, Euler and Navier-Stokes equations, upwind scheme, time-marching scheme

1. Introduction

The turbomachinery flows are among the most complex flows encountered in gas dynamics. They are dominated by convection effects and hence they can be defined at first approximation by the solution of Euler equation. Though they do not cover the influence of viscosity, still, they enable the analysis of the flow with discontinuities characteristic for transonic flows which commonly occur in heavy-loaded compression and expansion cascades (compressors and heat turbines). Many basic flow processes in turbomachines are characterised by high Reynolds numbers. The convection and diffusion effects approximated by the Navier-Stokes equations allow for the analysis of complicated flow phenomena and the losses level.

For these reasons the analysis of turbomachinery components has become increasingly dependent on the solution of the Navier-Stokes equations. The accuracy of the computational scheme depends on the discretisation error in space and in time and on the turbulence model applied. Information about advantages and disadvantages of various numerical codes for solution of the Euler equation is important also since they constitute an important element of each integration algorithm of viscous flow equations.

Through last years many algorithms for calculation of the inviscid flows or of the inviscid part in viscous flows, based on the central and upwind differencing have been developed. These algorithms are both equivalent, when to the central scheme some artificial dissipative terms are added. The upwind methods combine the type of differential operators with the directions of disturbance expan sion in the flow. In the case of the convection effects it allows for reduction of numerical dissipation and better modelling of discontinuities in the flow. For these reasons the group of the upwind type methods, covering a variety of approaches, in which the flux vector splitting and flux difference splitting are the most popular, recently has intensively developed. The flux difference splitting methods cover a large category of the so-called Godunov-type methods. This kind of the differencing schemes evolved from the original idea proposed by Godunov (1959), who first applied the solution of the initial-value Riemann problem to the numerical solution of conservation equations. Various versions of this approach: e.g., Godunov (1976), Osher and Solomon (1982), Roe (1981), Pandolffi (1984) constitute a basis for many specific solution algorithms of the Euler and Navier-Stokes equations.

The upwind Godunov-type methods are the first order accurate, monotone scheme. This leads to a poor representation even of linear phenomena. It is therefore essential to look for higher order schemes, to reduce the diffusive character of the first order schemes. The transfer to the high resolution Total Variation Diminishing (TVD) schemes makes this schemes very attractive for the analysis of transonic and supersonic flows in turbomachinery cascades. The TVD-schemes can be applied as to the Euler equations as to evaluation of the inviscid terms of the Navier-Stokes equations (Chakravarthy and Osher, 1985). According to the studies of van Leer et al. (1987) and Vatsa et al. (1987) it was found that built-in numerical dissipation terms introduced by highly accurate TVD-schemes based on the Riemann solvers automatically become small in boundary layers, so as not to dominate the natural diffusion. In this paper the numerical experiments to compare the calculation results of blade cascade 3D inviscid flows obtained applying the schemes with different degrees of accuracy are presented.

The Reynolds averaged Navier-Stokes equations solved for the turbomachi-

nery cascade flows required turbulence modelling. Various turbulence models have been developed in last years. The two-equation models or other complex turbulence models do not guarantee yet good modelling in all cases. In this algorithm the algebraic two-layer eddy-viscosity model developed by Baldwin and Lomax (1978) is used. Its simplicity makes it attractive while it was successfully tested on the many examples. This method has been still widely used in both external and internal flows, especially for the two- and three-dimensional engineering applications (e.g. Benetschik (1991), Merz et al. (1995)).

2. Governing equations for inviscid and viscous calculations

The equations of the fluid motion can be presented as follows

$$\frac{\partial \boldsymbol{Q}}{\partial t} + L(Q) = \boldsymbol{H} \tag{2.1}$$

The operators $L(Q)$ and values $\boldsymbol{H}$ depend on the flow model, form of dependent variables of the vector Q and coordinate systems applied.

For the 3D motion of the inviscid, compressible fluid Eqs (2.1) can be described by the Euler equations in the coordinate system rotating with the angular velocity $(\Omega, 0, 0)$ where Ω is a component placed in the axis x of the machine, as

$$\frac{\partial}{\partial t}\boldsymbol{Q} + \frac{\partial}{\partial x}\boldsymbol{E}' + \frac{\partial}{\partial y}\boldsymbol{F}' + \frac{\partial}{\partial z}\boldsymbol{G}' + \boldsymbol{H} = \boldsymbol{0} \tag{2.2}$$

where

$$\boldsymbol{Q} = \begin{bmatrix} \rho \\ \rho u \\ \rho v \\ \rho w \\ e \end{bmatrix} \qquad \boldsymbol{E}' = \begin{bmatrix} \rho u' \\ \rho u u' + p \\ \rho v u' \\ \rho w u' \\ e u + p u' \end{bmatrix} \qquad \boldsymbol{F}' = \begin{bmatrix} \rho v' \\ \rho u v' \\ \rho v v' + p \\ \rho w v' + p \\ e v' + p v \end{bmatrix}$$

$$\boldsymbol{G}' = \begin{bmatrix} \rho w' \\ \rho u w' \\ \rho v w' \\ \rho w w' + p \\ e w' + p w \end{bmatrix} \qquad \boldsymbol{H} = \begin{bmatrix} 0 \\ 0 \\ -\rho w \Omega \\ \rho v \Omega \\ 0 \end{bmatrix}$$

where

ρ	–	density
u, v, w	–	velocity components in the absolute frame of reference
u', v', w'	–	velocity components in the relative frame of reference
e	–	total energy per unit volume.

The static pressure for the perfect gas is defined by:

$$p = (\gamma - 1)\left[e - \frac{1}{2}\rho(u^2 + v^2 + w^2)\right] \tag{2.3}$$

where γ is the ratio of specific heats.

Preserving the same vector of dependable variables Q in Eqs (2.2) in absolute and relative frames of reference facilitates solution of the flow problem in the systems containing stator and rotor passages.

The transformation to the general curvilinear coordinate system (ξ, η, ζ) with the determinant of Jakobi matrix $J = |\partial(x, y, z)/\partial(\xi, \eta, \zeta)|$ gives

$$\frac{\partial}{\partial t}\hat{\boldsymbol{Q}} + \frac{\partial}{\partial \xi}\hat{\boldsymbol{E}} + \frac{\partial}{\partial \eta}\hat{\boldsymbol{F}} + \frac{\partial}{\partial \zeta}\hat{\boldsymbol{G}} + \hat{\boldsymbol{H}} = \boldsymbol{0} \tag{2.4}$$

where

$$\hat{\boldsymbol{Q}} = J\begin{bmatrix} \rho \\ \rho u \\ \rho v \\ \rho w \\ e \end{bmatrix} \qquad \hat{\boldsymbol{E}} = J\begin{bmatrix} \rho U' \\ \rho u U' + \xi_x p \\ \rho v U' + \xi_y p \\ \rho w U' + \xi_z p \\ e U' + pU \end{bmatrix} \qquad \hat{\boldsymbol{F}} = J\begin{bmatrix} \rho V' \\ \rho u V' + \eta_x p \\ \rho v V' + \eta_y p \\ \rho w V' + \eta_z p \\ e V' + pV \end{bmatrix}$$

$$\hat{\boldsymbol{G}} = J\begin{bmatrix} \rho W' \\ \rho u W' + \zeta_x p \\ \rho v W' + \zeta_y p \\ \rho w W' + \zeta_z p \\ e W' + pW \end{bmatrix} \qquad \hat{\boldsymbol{H}} = \begin{bmatrix} 0 \\ 0 \\ -\rho w \Omega \\ \rho v \Omega \\ 0 \end{bmatrix}$$

In these equations the contravariant relative velocity components are described as

$$\begin{aligned} U' &= \xi_x u + \xi_y(v + \Omega z) + \xi_z(w - \Omega y) \\ V' &= \eta_x u + \eta_y(v + \Omega z) + \eta_z(w - \Omega y) \\ W' &= \zeta_x u + \zeta_y(v + \Omega z) + \zeta_z(w - \Omega y) \end{aligned} \tag{2.5}$$

and the contravariant absolute velocity components as

$$\begin{aligned} U &= \xi_x u + \xi_y v + \xi_z w \\ V &= \eta_x u + \eta_y v + \eta_z w \\ W &= \zeta_x u + \zeta_y v + \zeta_z w \end{aligned} \tag{2.6}$$

This form of the Euler equations is useful for construction of the numerical algorithm for the turbomachinery calculations, especially, when the stator and rotor are commonly considered.

Assuming for the viscous calculations the two-dimensional flow model, the Reynolds-averaged unsteady Navier-Stokes equations obtained from Eqs (2.1) are written in conservation law form as

$$\frac{\partial \boldsymbol{Q}}{\partial t} + \frac{\partial \boldsymbol{E}}{\partial x} + \frac{\partial \boldsymbol{F}}{\partial y} = \mathrm{Re}^{-1}\left(\frac{\partial \boldsymbol{E}_v}{\partial x} + \frac{\partial \boldsymbol{F}_v}{\partial y}\right) \tag{2.7}$$

where

$$\boldsymbol{Q} = \begin{bmatrix} \rho \\ \rho u \\ \rho v \\ e \end{bmatrix} \qquad \boldsymbol{E} = \begin{bmatrix} \rho u \\ \rho u^2 + p \\ \rho uv \\ u(e+p) \end{bmatrix} \qquad \boldsymbol{F} = \begin{bmatrix} \rho v \\ \rho uv \\ \rho v^2 + p \\ v(e+p) \end{bmatrix}$$

$$\boldsymbol{E}_v = \begin{bmatrix} 0 \\ \tau_{xx} \\ \tau_{xy} \\ u\tau_{xx} + v\tau_{xy} - q_x \end{bmatrix} \qquad \boldsymbol{F}_v = \begin{bmatrix} 0 \\ \tau_{xy} \\ \tau_{yy} \\ u\tau_{xy} + v\tau_{yy} - q_y \end{bmatrix}$$

In addition, the static pressure is given by

$$p = (\gamma - 1)\left[e - \frac{1}{2}\rho(u^2 + v^2)\right] \tag{2.8}$$

where γ is the ratio of specific heats.

Assuming the Stokes hypothesis the stress terms are given by

$$\begin{aligned} \tau_{xx} &= \frac{2}{3}\mu(2u_x - v_y) \\ \tau_{xy} &= \mu(u_y + v_x) \\ \tau_{yy} &= \frac{2}{3}\mu(2v_y - u_x) \end{aligned} \tag{2.9}$$

where μ is the viscosity. The heat fluxes q_x, q_y are defined as $q_x = -kT_x$, $q_y = -kT_y$, where k is the coefficient of thermal conductivity.

The Navier-Stokes Eqs (2.8) are transformed to the general curvilinear coordinate system (ξ, η) with the determinant of the Jakobi matrix $J = |\partial(x, y)/\partial(\xi, \eta)|$. The resulting equations written in the strong conservation law form are

$$J\frac{\partial \boldsymbol{Q}}{\partial t} + \frac{\partial \hat{\boldsymbol{E}}}{\partial \xi} + \frac{\partial \hat{\boldsymbol{F}}}{\partial \eta} = \mathrm{Re}^{-1}\left(\frac{\partial \hat{\boldsymbol{E}}_v}{\partial \xi} + \frac{\partial \hat{\boldsymbol{F}}_v}{\partial \eta}\right) \tag{2.10}$$

where the transformed fluxes take the form

$$\begin{aligned} \hat{\boldsymbol{E}} &= J\left(\frac{\partial \xi}{\partial x}\boldsymbol{E} + \frac{\partial \xi}{\partial y}\boldsymbol{F}\right) & \hat{\boldsymbol{F}} &= J\left(\frac{\partial \eta}{\partial x}\boldsymbol{E} + \frac{\partial \eta}{\partial y}\boldsymbol{F}\right) \\ \hat{\boldsymbol{E}}_v &= J\left(\frac{\partial \xi}{\partial x}\boldsymbol{E}_v + \frac{\partial \xi}{\partial y}\boldsymbol{F}_v\right) & \hat{\boldsymbol{F}}_v &= J\left(\frac{\partial \eta}{\partial x}\boldsymbol{E}_v + \frac{\partial \eta}{\partial y}\boldsymbol{F}_v\right) \end{aligned} \tag{2.11}$$

and the stress terms are given after transformation by the following expressions

$$\begin{aligned} \tau_{xx} &= \frac{2}{3}\mu[2(\xi_x u_\xi + \eta_x u_\eta) - (\xi_y v_\xi + \eta_y v_\eta)] \\ \tau_{xy} &= \mu(\xi_y u_\xi + \eta_x u_\eta + \xi_x v_\xi + \eta_x v_\eta) \\ \tau_{yy} &= \frac{2}{3}\mu[-(\xi_x u_\xi + \eta_x u_\eta) + 2(\xi_y v_\xi + \eta_y v_\eta)] \end{aligned} \tag{2.12}$$

With the Bussinesq eddy-viscosity approximation an effective viscosity μ has two distinct parts

$$\mu = \mu_l + \mu_t \tag{2.13}$$

where the subscripts l and t denote laminar and turbulent quantities respectively. The laminar viscosity depends on the temperature T and is modelled by Sutherland's law

$$\mu_l = \sqrt{T^3}\frac{1 + 110.4/T_\infty}{T + 110.4/T_\infty} \tag{2.14}$$

The algebraic turbulence model of Baldwin and Lomax (1978) is adopted to estimate the eddy viscosity μ_t.

The coefficients of thermal conductivity k have been replaced by assuming a constant Prandtl number and the heat fluxes are as follows

$$\begin{aligned} q_x &= -\frac{\mu}{\mathrm{Pr}}\frac{1}{\gamma - 1}(\xi_x T_\xi + \eta_x T_\eta) \\ q_y &= -\frac{\mu}{\mathrm{Pr}}\frac{1}{\gamma - 1}(\xi_y T_\xi + \eta_y T_\eta) \end{aligned} \tag{2.15}$$

with the following abbreviation

$$\frac{\mu}{\mathrm{Pr}} = \frac{\mu_l}{\mathrm{Pr}_l} + \frac{\mu_t}{\mathrm{Pr}_t} \tag{2.16}$$

where Pr_l, Pr_t are laminar and turbulent Prandtl numbers, respectively.

All equations are nondimensionalized by arbitrary reference quantities using the following formulae

$$\tilde{\rho} = \frac{\rho}{\rho_\infty} \qquad \tilde{u} = \frac{u}{a_\infty} \qquad \tilde{v} = \frac{v}{a_\infty} \qquad \tilde{e} = \frac{e}{\rho_\infty a_\infty^2}$$
$$\tilde{t} = \frac{t a_\infty}{l} \qquad \tilde{\mu} = \frac{\mu}{\mu_\infty} \qquad \mathrm{Re} = \frac{\rho_\infty l a_\infty}{\mu_\infty} \tag{2.17}$$

where

l – flowfield reference length

a – sonic velocity

and subscript ∞ denotes the total quantity.

3. Numerical algorithm

The algorithm used to solve the system of equations (2.12) is a time-marching Godunov-type method. The discretisation in space of the flow gradients was carried out using the node-centered finite volume method (Fig.1a). The explicit, first order accurate forward time integration is implemented. The algorithm for the viscous flow calculation consists of inviscid and viscous parts. The inviscid part is the same as for the calculation of the inviscid flow model.

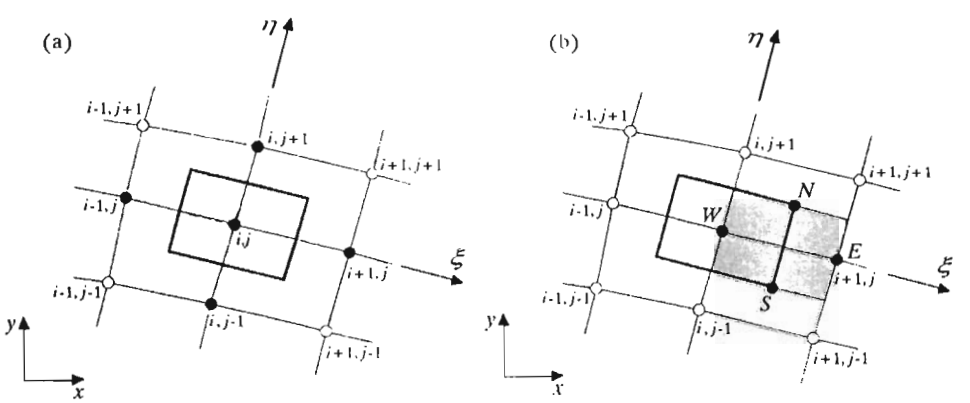

Fig. 1. Calculation cells; (a) node-centered basic cell, (b) special control volume for viscous fluxes

3.1. Integration in space

In the inviscid part the values of numerical fluxes on the surfaces bounding the numerical cell were calculated from the solutions of the local one-dimensional Riemann problems. This method requires:

- Defining the discrete (piecewise constant) values of conservative variables for time level t^n on each cell surface k necessary to formulate the local Riemann problems (left and right-hand initial states are the values $Q^L_{i+1/2}$ and $Q^R_{i+1/2}$ in the adjacent calculation cells)
- The exact or approximate solution of the 1D Riemann problem for the direction normal to the interface of the cell. In this paper for the inviscid 3D calculation the exact Riemann solver and for viscous calculations the approximate Roe solver were used. Detailed description of this solution is presented by Chmielniak and Wróblewski (1995), Chmielniak et al. (1995)
- Calculation of the numerical fluxes on the cell boundaries and obtaining the averaged solution in time t^{n+1}.

The diffusive terms are determined using a special central volume (Fig.1b). To construct the numerical viscous fluxes at the cell interfaces it is necessary to evaluate derivatives of the velocity components. They are treated following Chakravarthy (1988) and Benetschik (1991).

3.2. High order accuracy in space

The classical Godunov scheme leads to monotone algorithms of the first order accuracy in space. To obtain higher accuracy preserving monotonicity, van Leer's MUSCL approximation has been applied (see van Leer (1979), Hirsch (1990)) with the van Albada limiter function s (van Albada et al. (1982)). In this case, the vector of conservative variables is computed from the equation

$$
\begin{aligned}
Q^L_{i+1/2} &= Q_i + \left[\frac{s}{4}\Big((1-ks)\nabla_\xi Q + (1+ks)\Delta_\xi Q\Big)\right]_i \\
Q^R_{i+1/2} &= Q_{i+1} + \left[\frac{s}{4}\Big((1-ks)\Delta_\xi Q + (1+ks)\nabla_\xi Q\Big)\right]_{i+1}
\end{aligned}
\tag{3.1}
$$

The value ε was introduced to avoid division by zero ($\varepsilon = 10^{-5}$). For $k = 1/3$ we obtain the third order accuracy scheme. With the use of the flux limiter the scheme shows properties, which are similar to those of the TVD-schemes. The approximation (3.1) is valid for the uniform grid, otherwise, Q^L and Q^R are computed from (Benetschik (1991))

$$Q^L_{i+1/2} = Q_i + \left[\frac{s}{4}\left\{\left[\frac{\Delta l}{\nabla l} - k\left(2\frac{\Delta l}{\nabla l} - 1\right)\right]\nabla_\xi Q + \left[\frac{\nabla l}{\Delta l} + k\left(2 - \frac{\nabla l}{\Delta l}\right)\right]\Delta_\xi Q\right\}\right]_i$$

$$Q^R_{i+1/2} = Q_{i+1} - \left[\frac{s}{4}\left\{\left[\frac{\Delta l}{\nabla l} + k\left(2 - \frac{\Delta l}{\nabla l}\right)\right]\nabla_\xi Q + \left[\frac{\nabla l}{\Delta l} - k\left(2\frac{\nabla l}{\Delta l} - 1\right)\right]\Delta_\xi Q\right\}\right]_{i+1} \tag{3.2}$$

In Eqs (3.2) l means the local coordinate defined along the curve for which the interpolation is made. Operators Δ and ∇ are defined as in Eq (3.1). Interpolation can be defined for conservative or primitive variables.

3.3. Boundary conditions

The appropriate choice and the numerical implementation of boundary conditions are very important elements of the whole computation process. According to the theory of characteristics, three or four physical quantities for 2D or 3D calculations, respectively, should be prescribed at the subsonic inlet. The following are implemented: for 2D case – total temperature, total pressure and flow angle, and for 3D case the second flow angle is added. The value of Riemann invariant at the inlet boundary

$$R = \begin{cases} V' + \dfrac{2}{\gamma - 1}a & \text{for "C" – type grid}(\eta = \eta_{\max}) \\ U' - \dfrac{2}{\gamma - 1}a & \text{or "H" – type grid}(\xi = 0) \end{cases} \tag{3.3}$$

is determined on the basis of quantities defined for the internal cell adjacent to the boundary. For the supersonic inlet, all components are computed from the physical quantities prescribed on the boundary.

Only one physical variable is added at the subsonic outlet. For the turbomachinery calculations the static pressure is usually assumed. The remaining quantities are computed from the compatibility relations for Euler equations. In 3D calculations the radial distribution of static pressure at the outlet is calculated from the radial equilibrium equation.

Apart from the boundary conditions discussed, two types of internal conditions remain to be defined: conditions resulting from separation of one passage

(periodicity condition) and for stage calculations relations, defining the transfer from the stator frame of reference to the rotor one. In the first case, since the flow is examined in the reference system x, y, z, special attention should be paid to an appropriate transformation of component velocities. While defining conditions on the boundary line separating the stator from the rotor, one should use the standard boundary conditions at the inlet and outlet, as it was described above, taking into consideration the relationship between circumferentially averaged parameters in the absolute and the relative frames of reference.

For inviscid flow calculations the impermeability condition at solid walls is used. A detailed description of the boundary conditions used for the Euler equations are presented in Chmielniak and Wróblewski (1995). At solid walls the non-slip condition is used for the viscous flow calculation. The pressure is found using the high Reynolds-number approximation. For the grid orthogonal to the walls it is

$$\frac{\partial p}{\partial \eta} = 0 \tag{3.4}$$

Surface densities are computed from a specified wall temperature.

3.4. Computational grid

For the numerical calculations "C"-type and "H"-type grids are used. The "H"-type grid is generated by the algebraic method and used only for stage calculations. This makes calculation of the boundary condition in the stator/rotor interface simplier and is for the stage discretisation very popular (e.g. Merz et al. (1995)). Fig.2 presents the grid used for the stage calculations.

The grid generation procedure for the "C"-type grid is based on Poisson's equations according to the work of Sorenson (1980). This algorithm, which also reduces the grid skewing in the mid passage is very flexible. The periodic boundary conditions on the midgap boundary allows the computational mesh to adjust itself from the initial guess to make the mesh as orthogonal as possible in this region. As a result, the metrics of the computational grid remain continuous. The Dirichlet boundary conditions on the wall make the discretisation of the calculation domain close to the wall very fine and orthogonal, which is very important for the viscous flow calculations. Fig.3 presents the grid used for the viscous calculations.

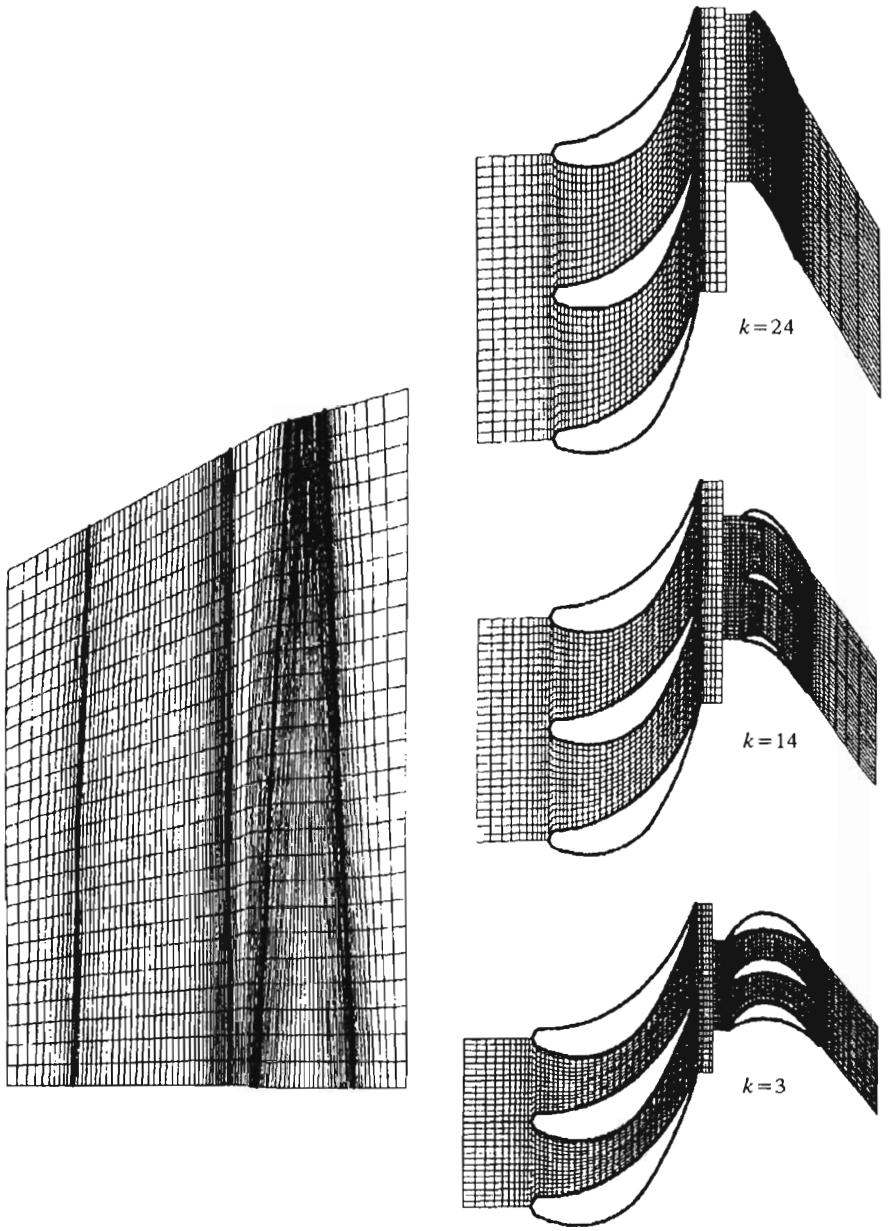

Fig. 2. "H"-type grid for the stage discretisation (k – grid surface number in r direction)

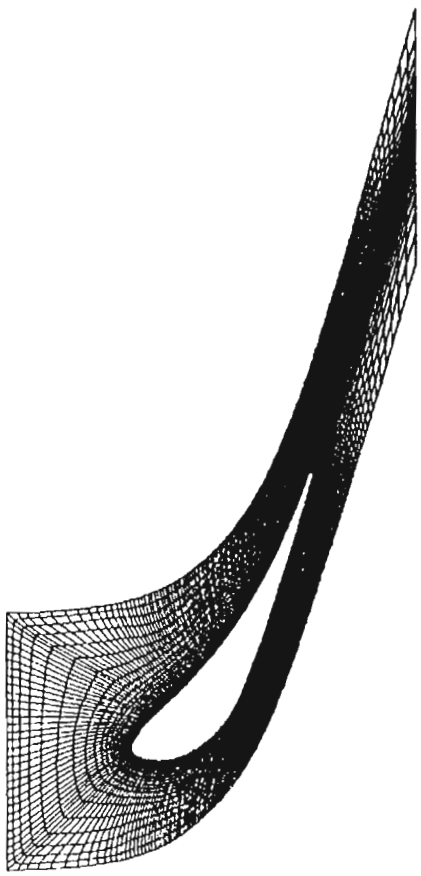

Fig. 3. "C"-type grid for the viscous flow computations

4. Numerical results

Calculation processes were performed on the examples of blade systems of steam turbines. The application of the Godunov-type scheme for real geometry of turbomachinery was presented, with the application of various methods of discretisation and inviscid and viscous flow models.

4.1. 3D inviscid flow calculations

Stator of the turbine (case 1)

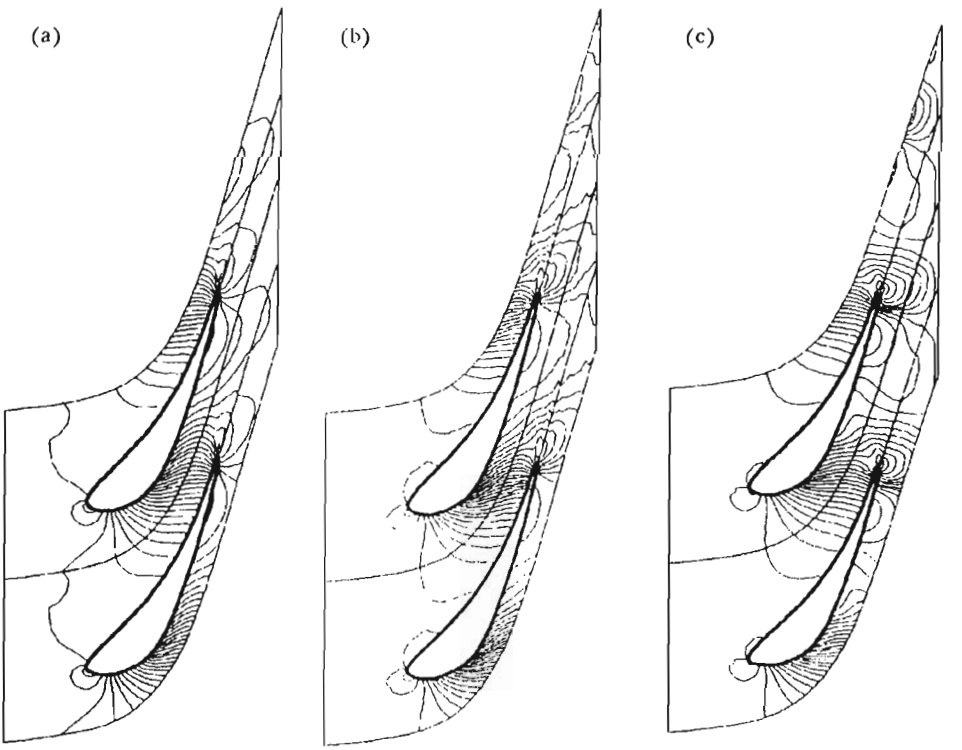

Fig. 4. Static pressure distribution; (a) for the coarse grid and the first order accuracy scheme, (b) for the coarse grid and the third order accuracy scheme, (c) for the fine grid and the third order accuracy scheme

For test computations, the geometry of turbine stator was chosen, for which the parameters and experimental results were presented by Bölcs et al. (1986). At the outlet, Mach number $Ma = 1.19$ was assumed. The numerical "C"-type grid applied to computations contained $101 \times 9 \times 21$ computation points for coarse grid and $201 \times 17 \times 21$ for fine grid. The distributions of static pressure on the blade in middle intersection of the blade high are presented in Fig.4. In the case of scheme of higher order, the structure of the resulting shock wave generated around the outlet edge is better, as it has been expected. The comparison of the distribution of Mach number on the profile shows considerable divergence of obtained results while applying

different orders of accuracy, Fig.5. The results for the first order of accuracy on the suction side differ considerably from the experiment results. The resolution improves in the case of scheme of higher accuracy order.

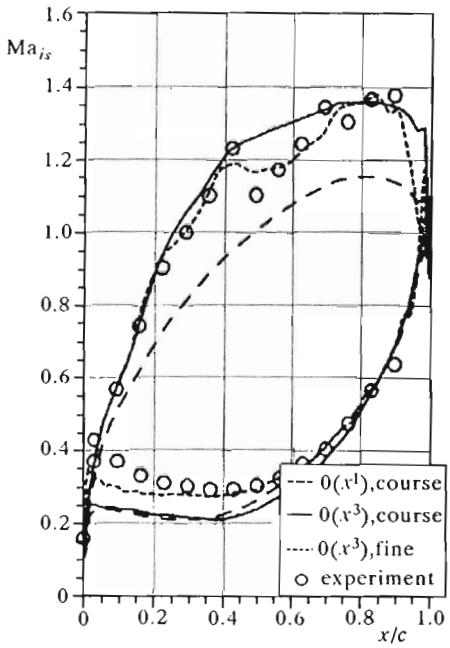

Fig. 5. Predicted and experimental Mach number distributions

Stator of the turbine (case 2)

The considered stator geometry belongs to the last stage of the steam turbine working in the area of the superheated steam. The superheated steam is treated approximately in the same way as a perfect gas. As it was in the previous case, the values of gas constants are assumed to be invariable in the whole area of the examined passage. The numerical grid applied to computations is of "H"-type, and it has $57 \times 17 \times 17$ points. The numerical grid is very short in the outlet area, which corresponds to the real configuration of the stator in the stage. Application of the classical boundary conditions at the inlet ($p(\Theta) = \text{const}$ for $r = \text{const}$) results in the elimination of shock wave formed around the outlet edge, when using the scheme of the first order of accuracy. The increase of computation accuracy leads in this case to the deterioration of convergence of the iteration process. The shock wave mode-

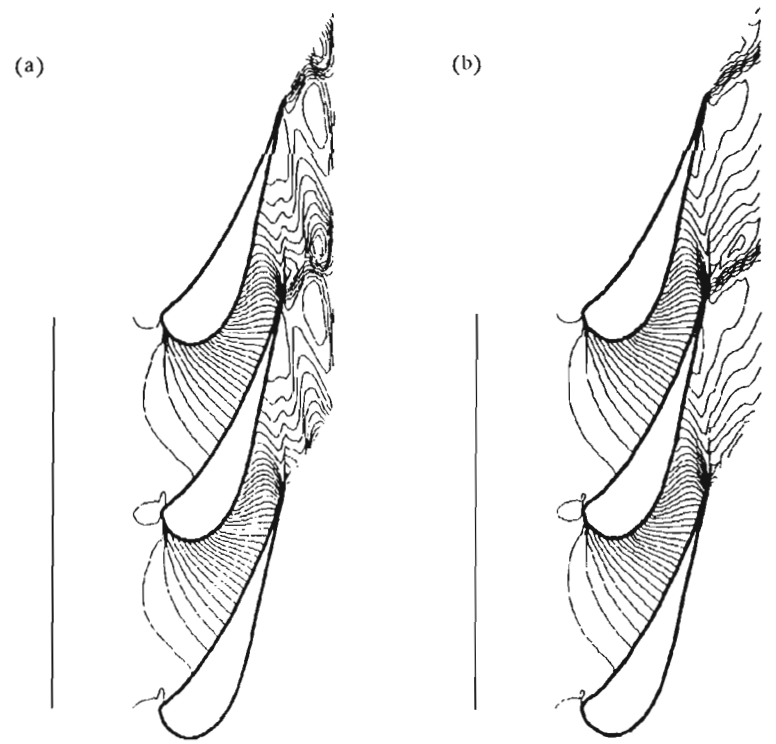

Fig. 6. Influence of boundary conditions on the static pressure distributions (3rd order accuracy); (a)constant static pressure at the outlet, (b) static pressure distribution at the outlet

led by the scheme of higher order of accuracy is in this case strong and it distinctly reflects against the outlet boundary (Fig.6a). Since the distance between the trailing edge of the profiles and the outlet boundary results in flow disturbances, oscillations are generated in this area. The applied numerical scheme makes it impossible to eliminate these oscillations. In this case, the modification of the outlet condition was applied, following the principle claiming that in the stage computations short areas at the outlet are considered a rule, so it is broadening will not solve the above problem in case of computations of the whole stage. The changed distribution of static pressure around the pitch was used as boundary condition; it was defined in such a way that its average value corresponds with the required p_{out} on a given radius. The circumferential distribution of the pressure at the outlet was defined on the basis of parameters from the internal part of computation area and it was corrected at each time step. The effects obtained in result of this modification

are presented in Fig.6b. Additionally, the improvement of convergence of the iteration process was observed.

Stage of the steam turbine

The computation of low through the blade system of two blade-rings was made for the geometry of the last stage of the steam turbine. The geometry of this stage is characterized by high blades and a small axial-ring gap. The calculations were carried out using the "H"-type, which contained $51 \times 15 \times 27$ computation nodes, both for the stator and rotor. For the computation, the numerical scheme of the third order of accuracy was applied. The stage under consideration works in the area of wet steam. For the computation some combination of state equations for the perfect and real gas was applied. Distributions of the static pressure in the stage are presented in Fig.7. The boundary conditions applied, with the parameteres defined in the axial gap, made it possible to eliminate smoothly transfers from the absolute to the relative coordinate system. Strong wave structures generated around the outlet edge of the stator are modeled in the way eliminating the occurrence of reflections against the outlet boundary. In the case of stage computations, the number of iterations to solve the Riemann problem at each grid cell face was controlled. When applying the optimal iteration process no more than 3 iterations were needed.

The application of the full Riemann problem requires longer computation time, but it may be attractive in the case of optimization of the iteration process and in the cases where strong wave phenomena occur, when detatiled calculation of entropy changes is required.

4.2. 2D viscous flow calculations

For the test computations a turbine cascade section was chosen. It is the fourth Standard Configuration proposed by Bölcs and Fransson (1986) for the workshop. This configuration was of interest mainly because it represents a typical section of modern turbine blades. This type of airfoil has relatively high blade thickness and chamber and operates under transonic flow conditions.

The cascade configuration consists of 20 blades, each with a chord of $c = 0.0744\,\mathrm{m}$ with the maximum thickness-to-chord ratio of 0.17. The stagger angle is 56.6° with the pitch-to-chord ratio of the cascade 0.76.

Experiments are performed for many conditions from which for comparison two are chosen. There are two different regimes of the work: subsonic with

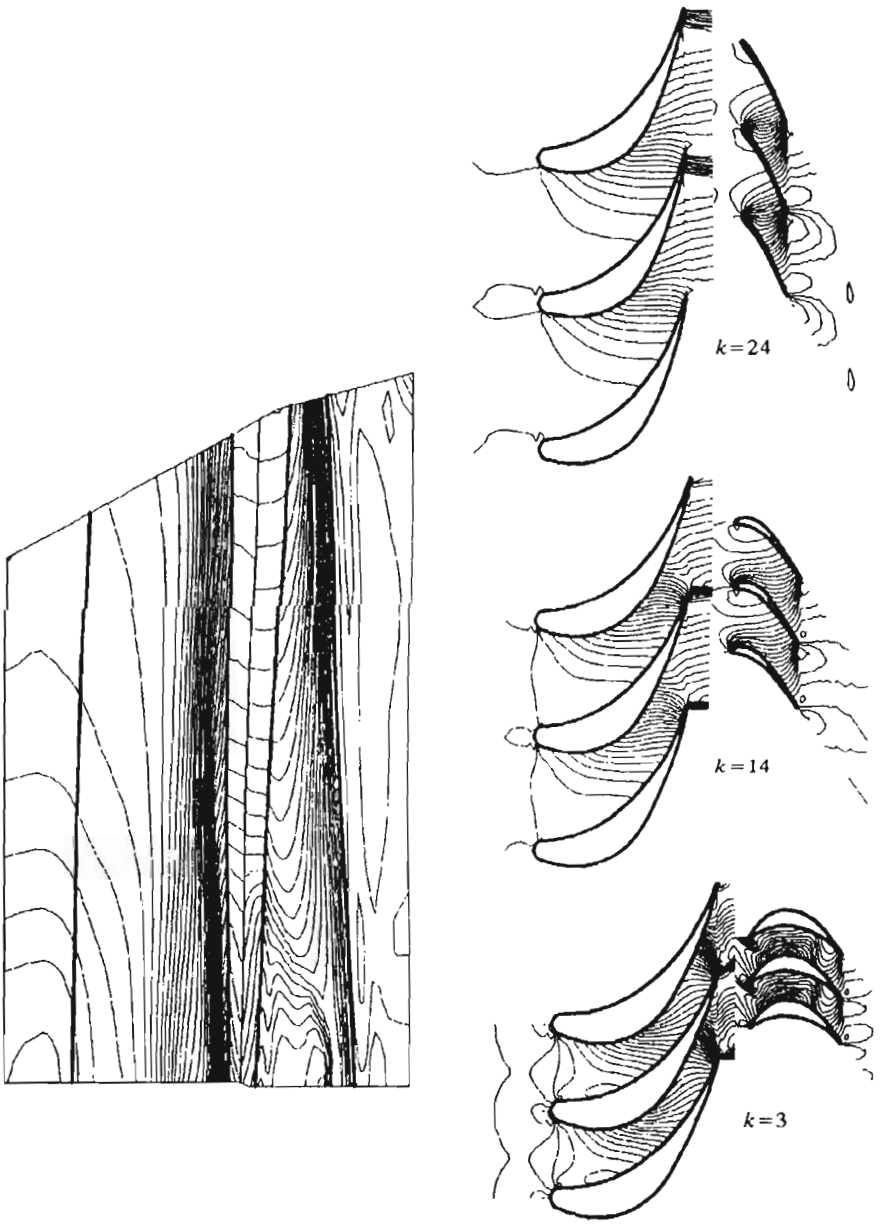

Fig. 7. Static pressure distributions for steam turbine stage (k-grid surface number in $r$direction)

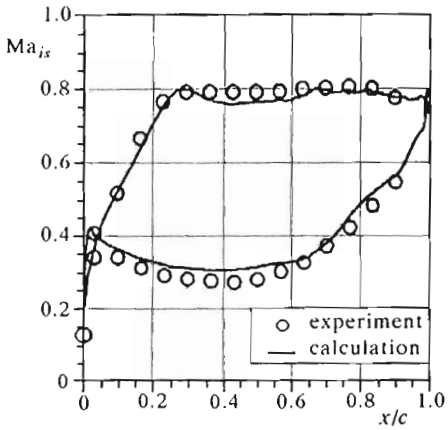

Fig. 8. Isentropic Mach number distribution, $Ma_{2is} = 0.72$

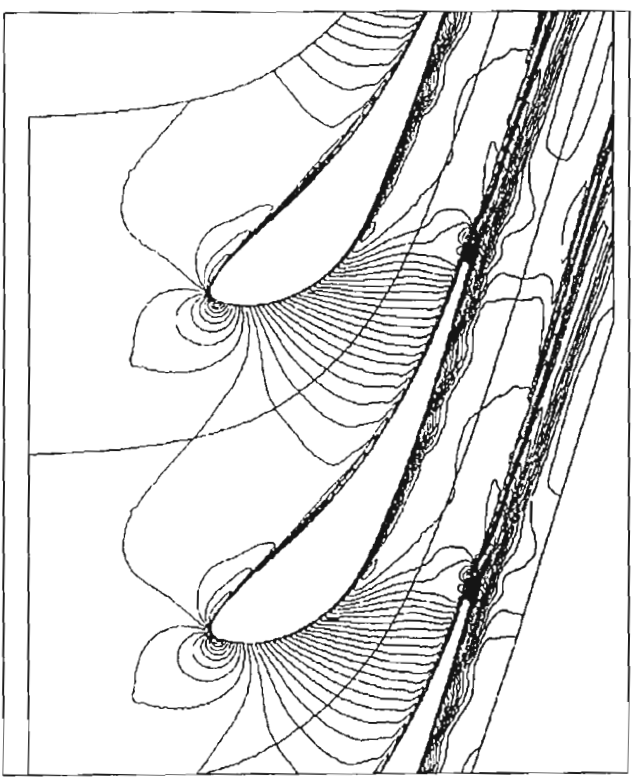

Fig. 9. Mach number contours, $Ma_{2is} = 0.72$

the isentropic Mach number at the outlet $Ma_{2is} = 0.72$ and transonic with the Mach number $Ma_{2is} = 1.19$.

The computations are performed using the "C"-type grid with 401×33 nodes (Fig.2). The minimum grid line distance from the wall was 0.03% of the chord length. In this case the chord Reynolds number based on the upstream conditions was $0.8 \cdot 10^6$, the Prandtl number and turbulent Prantdl number were 0.72 and 0.9, respectively.

Fig.8 shows the comparison of experimental isentropic Mach number distribution and computed results. The good agreement of the calculated data with the experimental ones is observed. Fig.9 shows the isolines of the Mach number distribution in the cascade.

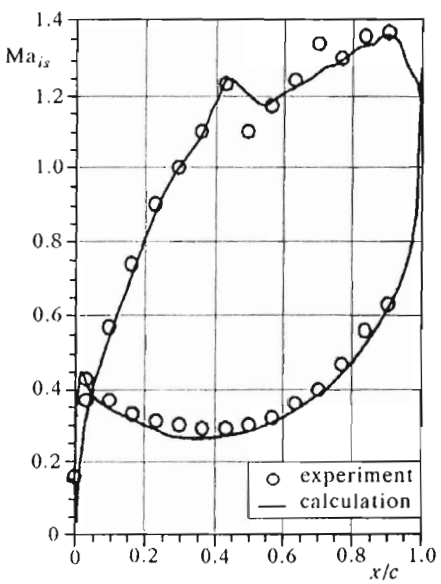

Fig. 10. Isentropic Mach number distribution, $Ma_{2is} = 1.19$

The calculations with the same parameters except for the exit isentropic Mach number equal 1.19 are performed. The isentropic Mach number distribution obtained from the calculation is compared with experimental data in Fig.10. It is easy to recognise that the agreement between the calculated and measured data at the pressure side of the blade is very good. In the transonic and supersonic ranges at the suction side the reflection of first shock wave generated at the trailing edge region is predicted well, but the second one is not present. This second shock wave reflection is obtained as a result of the

two earlier reflections: the first one from the suction side of the blade and the second one from the wake region. On the numerical grid using for calculations this second shock wave reflection at the suction side is smeared. The calculated isolines of Mach number are displayed in Fig.11.

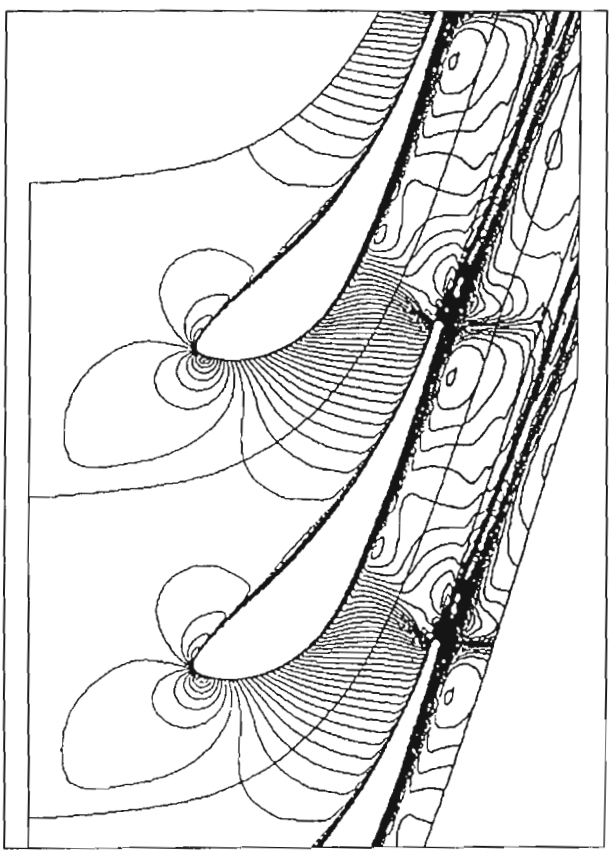

Fig. 11. Mach number contours, $Ma_{2is} = 1.19$

5. Conclusions

An Euler and Navier-Stokes analysis method for turbomachinery cascades has been presented. This method is based on an explicit time marching scheme. In the solution technique an upwind-biased discretisation of the in-

viscid fluxes thus avoiding additional artificial dissipation is used. The calculation is performed on the "H"-type grid and on the orthogonal "C"-type grid. The application of procedures of higher orders of accuracy to calculation of transonic flows better resolves the structure of discontinuity in the blade passages. The inviscid flow calculations show that the choice of scheme accuracy when the design problem is considered, could be very important. The increase of computation accuracy while examining the flow through the whole turbine stage requires the modification of boundary conditions in the stator/rotor intersection due to the occurrence of strong wave phenemena, to ensure convergence of the computation process. Such a modification eliminates unphysical disturbances of parameters in the small axial gap, which is necessary to compute the stationary flow through the stages.

The viscous flow calculations are made on the orthogonal "C"-type grid with implementation of the Baldwin-Lomax eddy-viscosity turbulence model. The accuracy of the computed solutions has been evaluated with experimental wall isentropic Mach numbers. The results of these comparisons led to the conclusion that the present method for solving the Navier-Stokes equations is capable of yielding accurate solutions for the flow in turbine cascades. For better prediction of the shock wave reflections future investigations must concentrate on the grid generation procedure that is one of the most important part of the numerical algorithm. One of the important task for the next work will be also implementation in this scheme one of the acceleration techniques.

References

1. BALDWIN B.S., LOMAX H., 1978, Thin Layer Approximation and Algebraic Model for Separated Turbulent Flows, *AIAA Paper*, 78-257

2. BENETSCHIK H., 1991, Numerische Berechnung der Trans- und Überschallströmung in Turbomaschinen mit Hilfe eines impliziten Relaxationsverfahren, Dissertation, RWTH Aachen

3. BÖLCS A., FRANSSON T.H., 1986, Aeroelasticity in Turbomachines. Comparison of Theoretical and Experimental Cascade Results, Communication du Laboratoire de Thermique Appliqu ee et de Turbomaschines de l'Ecole Polytechnique Federale de Lousanne, No.13

4. CHAKRAVARTHY S.R., OSHER S., 1985, A New Class of High Accuracy TVD Schemes for Hyperbolic Conservation Laws, *AIAA Paper*, 85-0363

5. CHAKRAVARTHY S.R., 1988, High Resolution Upwind Formulations for the Navier-Stokes Equations, *VKI LS*, 1988-05

6. CHMIELNIAK T.J., WRÓBLEWSKI W., 1995, Application of High Accuracy Upwind Schemes to Numerical Solution of Transonic Flows in Turbomachinery Blade Passages, *VDI-Berichte*, 1185, 63-77

7. CHMIELNIAK T.J., WRÓBLEWSKI W., DYKAS S., 1995, Comparision of the Godunov-Type Methods Using for the Transonic Internal Flow Computations, *Cieplne Maszyny Przeplywowe*, 108, Wyd. Politechniki Łódzkiej, 89-98

8. GODUNOV S.K., 1959, A Difference Scheme for Numerical Computation of Discontinuous Solution of Hydrodynamic Equations, (in Russian), *Math. Sbornik*, 47, 271-3062

9. GODUNOV S.K., 1976, *Numerical Solution of Multidimensional Fluid Dynamic Equations* (in Russian), Nauka, Moscow

10. HIRSCH C., 1990, *Numerical Computation of Internal and External Flows*, John Wiley and Sons, Chichester

11. MERZ R., KRÜCKELS J., MAYER J.F., STETTER H., 1995, Influence of Grid Refinement on the Solution of the Three-Dimensional Navier-Stokes Equations for Flow in a Transonic Turbine Stage with Tip Gap, *VDI-Berichte*, 1185, 211-224

12. OSHER S., SOLOMON F., 1982, Upwind Difference Schemes for Hyperbolic Systems of Conservation Laws, *Mathematics of Computation*, **38**, 158, 339-374

13. PANDOLFI M., 1984, A Contribution to the Numerical Prediction of Unsteady Flows, *AIAA Journal*, **22**, 5, 602-610

14. ROE P.L., 1981, Approximate Riemann Solver, Parameter Vector and Difference Schemes, *Journal of Comp. Phisics*, **34**, 357-37

15. SORENSON R.L., 1980, A Computer Program to Generate Two-Dimensional Grids About Airfoils and Other Shapes by the Use of Poisson's Equation, NASA TM-81198

16. VAN ALBADA G.D., VAN LEER B., ROBERTS W.W., 1982, A Comparative Study of Computational Methods in Cosmic Gas Dynamics, *Astron. Astrophysics*, 108, 76-84

17. VAN LEER B., 1979, Towards the Ultimate Conservative Difference Scheme. V. A Second order Sequel to Godunov's method, *Journal of Computational Physics*, **32**, 101-136

18. VAN LEER B., THOMAS J.L., ROE P.L., NEWSOME R.W., 1987, A Comparison of Numerical Flux Formulas for the Euler and Navier-Stokes Equations, *AIAA Paper*, 87-1104

19. VATSA V.N., THOMAS J. L., WEDON B.W., 1987, Navier-Stokes Computations of Prolate Spheroids at Angle of Attack, *AIAA Paper*, 87-2627

Obliczenia przepływu transonicznego z wykorzystaniem schematów typu Godunowa

Streszczenie

W artykule przedstawiono metodę rozwiązania równań Eulera dla przestrzennego przepływu w kierowniczym kanale lopatkowym i w stopniu turbinowym oraz metodę rozwiązania równań Navier-Stokes'a dla dwuwymiarowego przepływu w kanałach lopatkowych maszyn wirnikowych. Do obliczeń zastosowano jawną metodę objętości skończonych z komórkami bilansowymi typu "node-centered". Dyskretyzacja członów nielepkich równań zachowania dokonana została za pomocą schematów typu Godunowa z dokładnym i przybliżonym rozwiązaniem zagadnienia Riemanna. Schematy te są schematami typu "upwind" i pozwalają na prowadzenie obliczeń dla szerokiego zakresu prędkości czynnika: od poddźwiękowej do naddźwiękowej. W celu otrzymania wyższego rzędu dokładności w przestrzeni zastosowano aproksymację typu MUSCL. Do modelowania turbulencji zastosowano algebraiczny model Baldwin'a-Lomax'a. Obliczenia prowadzono na ortogonalnej siatce typu "C" wygenerowanej w oparciu o rozwiązanie równań Poisson'a oraz w przypadku obliczeń stopnia na algebraicznej siatce typu "H". Omówiono wyniki obliczeń przepływu w kanałach lopatkowych turbin osiowych i porównano z dostępnymi w literaturze badaniami eksperymentalnymi.

Manuscript received October 8, 1996; accepted for print January 10, 1997